

# New Factors of Reliability of Electric Furnaces for Vermiculite Firing with Mobile Base Plates



Anatoliy Nizhegorodov, Aleksey Gavrilin, Boris Moyzes, Kirill Kuvshinov, and Saule Sakipova

**Abstract** The article reviews measures to increase the reliable operation of electric furnaces for vermiculite concentrates firing over the entire period of their existence since 2003. A significant step forward in this research was the find that the implementation of suspended heating systems in the electric modules of furnaces, both types such as modular-triggering furnaces and in furnaces with mobile base plates, where the swelling process of the raw material is carried out during the process of its vibrotransportation in the thermal field of the heating system. The imbalance of inertial loads is an additional factor for reducing of operation reliability in furnaces with mobile base plates. The methods of their balancing, discussed in this research, provide the dynamic balance of all moving parts of these furnace units. A study of analytical models of temperature distribution, carried out in previous researchers of the authors, showed that uniform heating can only be achieved in systems with a variable interval for the placement of heaters. The research results carried out in this work at the accepted values of the minimum and maximum intervals show that,

---

A. Nizhegorodov

Department of Construction and Road-Making Machines and Hydraulic Systems, Irkutsk National Research Technical University, 83 Lermontov Street, Irkutsk, Russia 664074  
e-mail: [nastromo\\_irkutsk@mail.ru](mailto:nastromo_irkutsk@mail.ru)

A. Gavrilin · K. Kuvshinov

Division for Materials Science, National Research Tomsk Polytechnic University, 30 Lenin Avenue, Tomsk, Russia 634050  
e-mail: [tom-gawral@list.ru](mailto:tom-gawral@list.ru)

K. Kuvshinov

e-mail: [kuvshinov@tpu.ru](mailto:kuvshinov@tpu.ru)

B. Moyzes (✉)

Division for Testing and Diagnostics, National Research Tomsk Polytechnic University, 30 Lenin Avenue, Tomsk, Russia 634050  
e-mail: [mbb@tpu.ru](mailto:mbb@tpu.ru)

S. Sakipova

Physical and Technical Faculty, E.A. Buketov Karaganda University, 56 Ave. Nursultan Nazarbayev, Karaganda 100027, Kazakhstan  
e-mail: [sesaule@mail.ru](mailto:sesaule@mail.ru)

© The Author(s), under exclusive license to Springer Nature Switzerland AG 2021

125

I. V. Minin et al. (eds.), *Progress in Material Science and Engineering*,  
Studies in Systems, Decision and Control 351,  
[https://doi.org/10.1007/978-3-030-68103-6\\_12](https://doi.org/10.1007/978-3-030-68103-6_12)

compared to the old systems located on the refractory base of the firing modules, the difference temperature decreases significantly, which proves the effectiveness of this approach.

## 1 Introduction

Constant work was being made by the improving of the electric modular launch furnaces for firing vermiculite concentrates and conglomerates since their introduction. The need to reduce the specific energy consumption of firing and increase their reliability remained relevant [1–6]. Modular-launch furnaces made it possible to achieve the minimum energy intensity of 170–175 mJ/m<sup>3</sup> [7], but due to a number of design aspects (the use of inclined modules with accelerating movement of raw materials, etc.), further reduction was not achieved.

Then an alternative concept of operation units for vermiculite firing (and other thermally activated bulk materials [8]) appeared. They were the electric furnaces with mobile base plates, which made it possible to bring the specific energy consumption of firing to 60–70 mJ/m<sup>3</sup>.

The special features of new improved electric furnaces design are the follows:

- it allows to minimize operating space of the firing modules;
- implementation of quick-detachable suspension heating systems;
- it allows to transport the fired raw materials in the thermal field of the modules at a constant speed with a continuous flow of vermiculite concentrate particles [9–11].

These features make it possible to achieve high energy efficiency as well as make the units more competitive and help to operate at a their maximum reliability level.

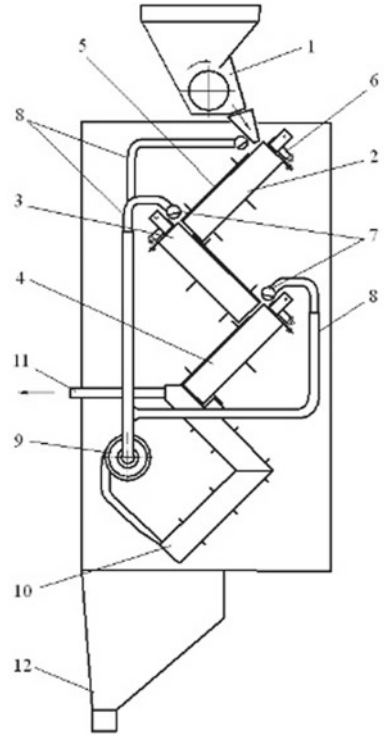
The purpose of this work is to increase the reliability of the electric furnaces under consideration through the use of a new design of quick-detachable heating systems and dynamic balancing of the base plates [12–15].

## 2 Reliability Factors of Electric Furnaces for Vermiculites Firing

The experience gained during the production operation of the first modular-launch furnaces at the Kvalitet LLC enterprise in the city of Irkutsk made it possible to identify the causes of failures and find effective technical solutions that increased the reliability of their operation.

For example, let's consider a three-module furnace with an additional “zero” non-electrified module (Fig. 1).

**Fig. 1** Three-module furnace with an additional “zero” non-electrified module



Vermiculite mica concentrate supplied by dispenser 1 passes through electric firing modules 2, 3, and 4, closed by thermo-covers 5. Using fastening heads 6, strip-type electric heaters with a surface heating temperature of 740–780 °C are installed on the edge of the modules. The strip-type electric heaters form longitudinal chambers (Fig. 2a), where vermiculite moves, being exposed to thermal radiation from both sides.

In the first design of the furnace, the heaters were located not on the edge, but flat, as it shown in Fig. 2b. Although the efficiency of transferring thermal energy to

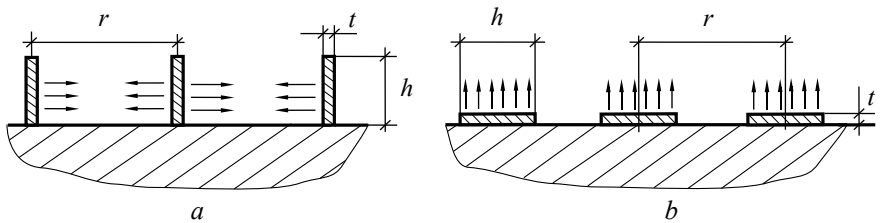


**Fig. 2** Methods of installing strip electric heaters: *a*—on the edge, *b*—flat, *r*—installation step, *t*—thickness, *h*—width of heaters

**Fig. 3** Soot deposit on strip heaters during firing concentrates of the Tatar deposit of vermiculite ores



expanded vermiculite in this method was somewhat greater, the failure rate of the furnace was very high due to the soot deposit (Fig. 3).

Suction pumps 7 (Fig. 1) located in the upper end parts of the modules, are connected by pipelines 8 with an exhaust fan 9. Due to the temperature difference and air traction that occurs in the slit-like spaces of the firing modules, the fine particles of vermiculite formed during its expansion are ejected and trapped suction pumps. A stream of hot air saturated with vermiculite dust passes through an additional module 10, heating it, and is discharged into the dust deposition and air purification system through the pipe 11.

The upper modules 2, 3 and 4 are connected sequentially, and the third lower electrical module is tightly attached to the “zero” module 10. The “zero” module 10 allows to use thermal exergy accumulated by vermiculite in electrical modules and the thermal radiation of small particles of vermiculite to complete the mechanical transformation (structure formation) of vermiculite at the absence of an external heat source. The tests results proved [4], that the use of such modules can reduce the energy consumption and energy intensity of firing by 10–20%.

The expanded product is poured into the hopper 12.

Failures in the operation of furnaces decreased significantly when heaters were installed on the edge, but this was only one of the factors of low reliability. There were congestions, the vermiculite flow stopped in the operating chambers because of the fragments collapse of the asbestos lining of thermal covers 5. It led to local overheating of the heaters and their burnout.

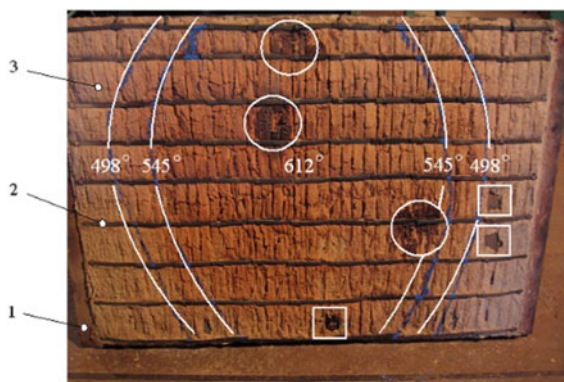
Another cause of failure was the interturn circuit due to the ingress of conductive objects into the furnace along with vermiculite concentrate.

We used felt as a thermally insulator for mullite-siliceous module covers, which is capable to maintain its properties at temperatures above 1380 °C. Application of felt allowed us to avoid the collapse of lining. Also any foreign objects were prevented to occur in the furnaces by pre-fractioning concentrates in drum sieves [8].

But all these measures reduced the failure rate by only 55–60%.

It turned out that the operation of the heating systems of the firing modules does not provide uniform heating of the refractory surfaces of the modules where the expanded vermiculite rolls. Obviously, for the same interval  $r$  of arrangement of heating elements (Fig. 2) the temperature in the central part of the module and on its

**Fig. 4** Thermocover of the firing module: bottom view: 1—steel base, 2—lining fastening by strip nichrome, 3—lining of asbestos cord



periphery cannot be the same. Several researchers conducted studies and published works [16, 17], on the analytical models of the temperature distribution both on the refractory surface of the module and on the surface of the thermal cover. The temperature measurements were also taken on the surface of the thermal cover of one of the modules of the operating furnace. Figure 4 shows a thermal cover that has been in operation process at least 140 h. Here, the white lines indicate the approximate position of the isotherms with temperatures of 498 and 545 °C and the temperature in its central part 612 °C. Radiant energy flows from heaters and leaves traces which indicate that the temperature distribution is uneven on the refractory surface of the module. White circles outline the places where nichrome melted (1420–1460 °C). The squares indicate the places of peeling and falling out of the lining fragments mentioned above.

It is also obvious that burning out of heating elements due to soot deposit is the most difficult problem to resolve. The burnout mainly occurs in the center of the module, where the temperatures are highest. The problem remained unresolved. The surfaces of the cover and base, and most importantly, the of the heaters themselves which located in the central part, are getting heated more severely. Vermiculite concentrate always contains a small amount of associated minerals which have a relatively low melting point (vermiculite itself melts at temperatures from 1150 to 1350 °C, depending on its natural properties [18]). Quality of enrichment does not change the melting temperature. So when nichrome is overheated, the associated minerals adhere to its surface and form soot deposits (Figs. 3 and 4).

The suspended heating system allows to solve this problem and radically raises the reliability of electric furnaces for vermiculite firing to a new level (Fig. 5).

The difference is provided by the heaters 2 which are located above the base plate 1 under the thermal cover 3 and are held by special fasteners that have locks 4, hooks 5 and clamps 6 and provide the heaters are held with the same gap in relation to the base plate entire length. The heaters do not come into contact with the expanded grains of vermiculite and emit thermal radiation both to the bottom, to the processed raw materials, and up to the well-insulated module cover. The movement of the

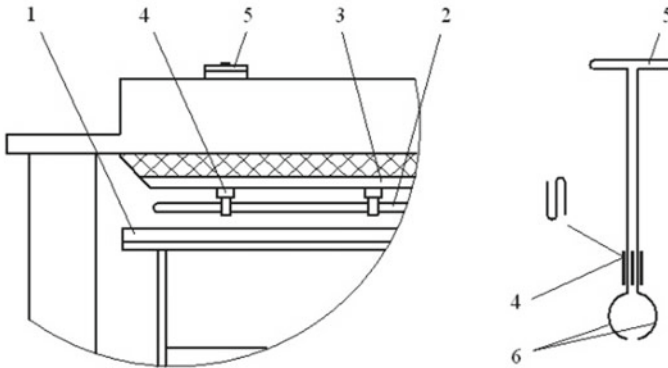


**Fig. 5** Suspended heating system of wire heaters: fragment of the furnace firing module with a mobile base platform

concentrate in the heat field of the heaters is provided by non-symmetric vibrations of the base plate [9].

Let's consider one of the design options for an industrial electric furnace, consisting of six firing modules placed in two sections and, using its example, those technical solutions that will radically improve the reliability of such a furnace unit.

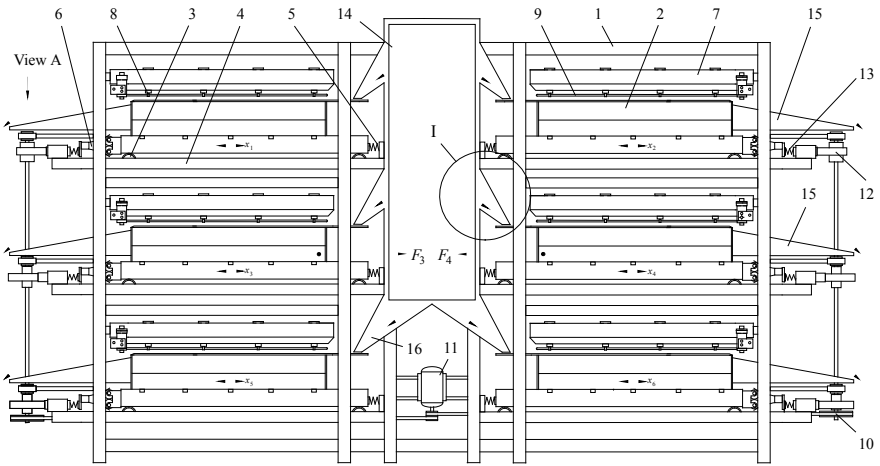
### 3 The Device of a Two-Section Six-Module Industrial Electric Furnace

Figure 6 shows a diagram of a two-section industrial furnace, consisting of six firing modules. It is a closed metal cabinet with insulated walls and door leaves (they are conventionally removed in Fig. 6). The furnace contains a common frame 1, mobile base plates 2 mounted on rollers 3 in the guide frames 4, spring-loaded on one side by coil springs 5 and non-linear elastic elements 6 on the other sides. Thermal covers 7 are mounted on modular units, and under them using special fasteners 8 are placed suspended electric heating grids 9.

Eccentric shafts are installed on each side of the furnace, which are driven through gear belt (or chain) gears 10 with a gear motor 11 with a rotation speed of 5–8 r/s.

The eccentrics 12 excites non-symmetrical vibrations of the base plates by means of tolls and springs 13 and with the help of non-linear elastic elements 6, which causes a vibro-transport effect [19] and provides one-way movement of vermiculite concentrate particles from the trays 16 of the hopper 14 under the heating grid 9 in the thermal field of the firing modules. The output of the expanded product occurs through trays 15.

In the process of oscillation of base plates, the significant inertia forces  $F$  occur. The forces  $F$  are determined by multiplying (N):  $F = m_i \cdot a$ , where  $m_i$ —is the mass



**Fig. 6** Two-section six-module industrial electric furnace

of the *i*-th base plate with all elements attached to it, *kg*, and *a*—its vibration acceleration,  $m/c^2$ .

The synchronism and phase balance of oscillations of each pair of base plates is provided by the installation of eccentrics with a displacement of one relative to the other by 120° (Fig. 7a). This balances their multidirectional inertia forces *T* (N):

$$T = m\omega^2 e,$$

where *m* is the mass of the eccentric, *kg*,  $\omega$  is the angular velocity of rotation of the shaft in rad/c, *e* is the eccentricity.

The inertia forces of the base plates *F* cause the high risk situation. These forces can lead to swinging of the entire furnace, to the appearance of sub- and super harmonics

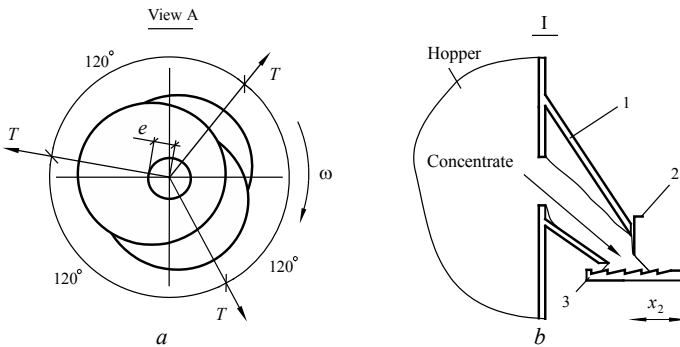


**Fig. 7** Installation of eccentrics on the drive shaft with an angular pitch of 120° (a) and a diagram illustrating the dosage of vermiculite concentrate (b)

of its individual elements, and, in particular, to the excitation of vibrations of the rods of the heating grids 9. If the dynamic equilibrium of the entire system is not provided, then resonances or amplitude-modulated oscillations of individual heaters, their contacts and short circuits will occur. This happened when testing of a physical model of a single-phase furnace with a mobile base plate [8].

For balancing the base plates of each level, the eccentrics making them move vibrationally are set towards each other, and their shafts are connected by gear belt (or chain) gears 10 to the gear motor 11. This provides synchronous and antiphase oscillations of the base plates so that peak values of inertia forces  $F_3$  and  $F_4$ , Fig. 6 are equal and directed oppositely. The dosing process of vermiculite concentrate in this furnace design is carried out from the common hopper through trays 1 equipped with adjustment flaps 2 using the base plates 3 themselves, due to the non-symmetry of their vibrations and the corrugated surface in zone "I" with a notch directed to the side of firing modules (Fig. 7b).

## 4 Results and Discussion

### 4.1 *Redistribution of Thermal Power and Temperature of the Heating System*

Let's turn to the main question about the distribution of thermal power and temperature of heaters in a suspended heating system (Fig. 5).

As it has been noted, burnout of heating elements due to soot deposit occurs most often in the central part of the module, where the temperatures are the highest. Not only the surfaces of the cover and refractory base, but also the heaters themselves, which are located in the central part, heat up more significantly. In the research [17] it is shown that in the pilot-industrial modular-firing furnace with belt heaters made of nichrome, the temperature differential was from 1119 °K in the center of the module to 910 °K along the sides with a discrepancy of 23%.

One heater 1 (Fig. 8) is an elongated U-shaped element of two rods, only here they are all made as a single heating grid with two ends for connection to the electrical network using fixing heads 2. The heaters are held by special clamps 3 under the thermal cover.

The design of the heating grid is such that the interval  $r_a$  between the rods of the first (extreme) heater  $a$  is half the interval  $r_b$  of the central heater  $b$ .

If there are only  $n$  intervals, then, on average, an increase in one interval between the rods will be (mm):

$$\Delta = \frac{r_b - r_a}{n}.$$



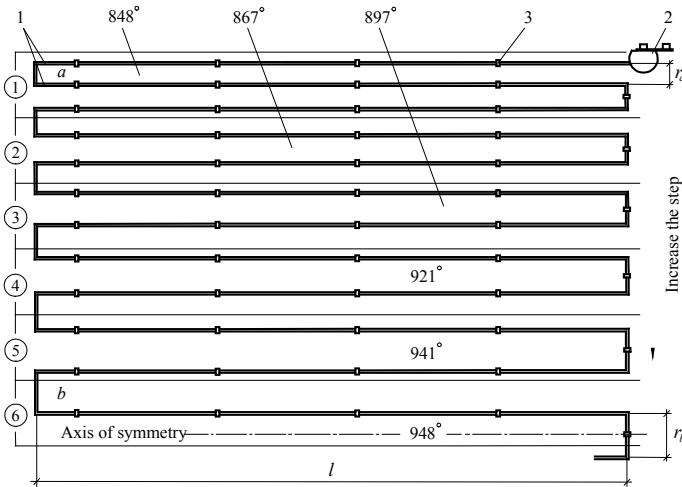


**Fig. 8** Heating grid with variable spacing between rods

Let's set the values of the intervals  $r_a = 22$  mm and  $r_b = 44$  mm. Then the increase in each interval at  $n = 11$  will be equal to  $\Delta = 2$  mm.

With a heater length  $l$  equals to 400 mm, the total length of the heating grid can be calculated (mm):

$$l_{\Sigma} = 24 \cdot l + 2 \cdot (11 \cdot r_a + 55 \cdot \Delta + r_b),$$

moreover, the term of the obtained expression  $2 \cdot (11 \cdot r_a + 55 \cdot \Delta + r_b)$ , will determine the width of the firing module, which in this case will be equal to 792 mm, and the total length of the heating grid—10,392 mm or 10.39 m.

All initial parameters:  $r_a = 22$  mm,  $r_b = 44$  mm,  $\Delta = 2$  mm,  $l = 400$  mm and  $n = 11$  are not taken by chance. The total length of 10.39 is approximately equal to the total length of the heaters of the prototype of the electric furnace with a mobile base plate. The experimental results are given in [20]. In this case, the cross-sectional area of the tape heaters was 10 mm<sup>2</sup>.

Then it can be taken the values of the current values of the current  $I = 79$  A and voltage  $U = 162$  V, at which the maximum productivity and minimum density of expanded vermiculite were achieved [8], to calculate the consumed electrical power (W):

$$N = I \cdot U = 79 \cdot 162 = 12798.$$

Let us determine the value of the specific power (referred to the total length) (W/m):

$$N_l = \frac{N}{l_\Sigma} = \frac{12798}{10.39} = 1232.$$

Neglecting the end sections of the heating grid ( $r_a$ ,  $r_a + \Delta \dots$  and  $r_b$ ), let's find the power per rod (W):

$$N_o = N_l \cdot l = 1232 \cdot 0.4 = 493. \quad (1)$$

The thermal power emitted by a single rod can be found by the formula obtained by the analytical method of balance fluxes [21] (W):

$$Q_o = [\varepsilon \sigma T_o^4 (1 + \rho_o \varphi_{o1}) + \rho_o Q_2 (\rho_o \varphi_{o1} \varphi_{21} + \varphi_{2o}) + \rho_o Q_3 (\rho_o \varphi_{o1} \varphi_{31} + \varphi_{3o})], \quad (2)$$

where  $\varepsilon$  is the nichrome heater blackness level,  $\sigma$  is the Stefan-Boltzmann constant [10],  $\rho_o$  is the reflectivity of the heater,  $\varphi_{o1}$ ,  $\varphi_{21}$ ,  $\varphi_{2o}$ ,  $\varphi_{31}$  and  $\varphi_{3o}$  are the angular coefficients that take into account the reflected radiation falling on a single heater, on the surface of the module base ( $\varphi_{2o}$ ), on the surface of the thermal cover ( $\varphi_{3o}$ ), to the adjacent heater from the surface of the thermal cover ( $\varphi_{21}$  и  $\varphi_{31}$ ),  $Q_2$  и  $Q_3$ —are the power of the heat reflected radiation from the surface of the base and thermal cover, respectively [22–25]. Taking into account the losses during the conversion of electrical power into heat, the heat power emitted by a single rod can be found using the Formula (1),

$$W : Q_o = 0.92 \cdot N_o, \quad (3)$$

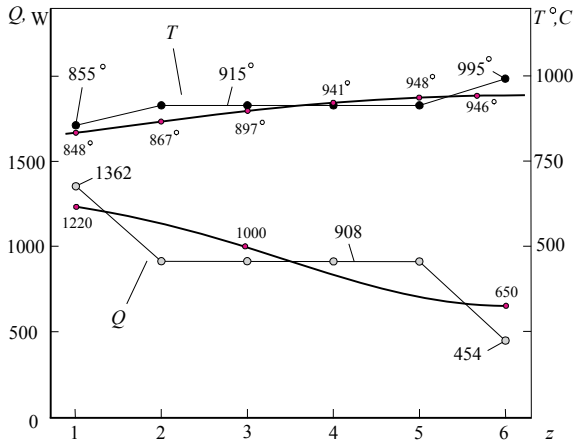
where 0.92 is the approximate value of the loss factor [21]. Then the thermal power determined by the Formula (3) will be equal to 454 W [26].

To determine the nature of the distribution of heat power, let us combine half of the heating grid (taking into account its symmetry) with the marking of the surface of the firing module in the form of zones 1, 2 ... 6 of the same size, circled (Fig. 8). Let's see how many heating rods will be in the indicated zones: 1st zone—three rods, 2nd zone—two rods, two rods in zones 3, 4 and 5, and in zone 6—one rod. This means that the first zone has 1362 W of thermal power, the second, third, fourth and fifth zones have 908 W each, and the sixth only 454 W.

Figure 9 shows the distribution of heat power by the indicated zones: broken line  $Q$ . But this is just a “zonal model”, because heat energy cannot be distributed discretely, therefore, a smoothing line with average values of heat power is shown here. In the first zone—1220 W, in the second, third, fourth and fifth zones—1000 W and in the sixth zone 650 W. It should be noted, that the indicated values of the average thermal power are radiation of the heaters into the surrounding space. Some of these flows fall on the base of the module and the thermal cover in its own zone, the rest to adjacent zones, including adjacent heaters [27–30].

So, in the structure of the Formula (2): its terms reflect:

**Fig. 9** Distribution of thermal power and heaters temperature by zones of their location (z is the ordinal number of the zone)



- $\varepsilon\sigma T_o^4 f \rho_o \varphi_1$ —is the fraction of reflected thermal radiation falling on the heating element from the surface of the adjacent heater;
- $\rho_o Q_2 (\rho_o \varphi_{o1} \varphi_{21} + \varphi_{2o})$ —is the fraction of the reflected thermal radiation falling on the heating element from the surface of the refractory base of the module;
- $\rho_o Q_3 (\rho_o \varphi_{o1} \varphi_{31} + \varphi_{3o}) - \rho_o Q_2 (\rho_o \varphi_{o1} \varphi_{21} + \varphi_{2o})$ —the fraction of the reflected heat radiation falling on the heating element from the surface of the module’s thermal cover.

It still does not take into account the flows of thermal radiation from distant heaters and the corresponding sections of the surfaces of the base and thermo-cover, which reach the surface of a single heater. But all these fractions of the reflected radiation, as shown by the calculations carried out in [17], are approximately 10–12% of the intrinsic radiation of the heater. Therefore, the calculation of heater temperatures was carried out using a simplified formula:

$$Q_o = \varepsilon\sigma T_o^4 f,$$

solved with respect to T, °K:

$$T = \left( \frac{Q_o}{\varepsilon\sigma T_o^4 f} \right)^{\frac{1}{4}}.$$

Figure 9 by the broken line at the top, shows the distribution of the average temperature values converted to degrees Celsius, three heaters in the first zone—855 °C, two heaters in zones 2, 3, 4 and 5—915 °C and one heater in the sixth zone—995 °C. And although the temperatures of the heaters just change discretely from one to the other, they cannot be the same in the second, third, fourth and fifth zones. To find the approximate values of the average temperatures of the heaters, a smoothing (averaging) line is shown here, indicating the average values of T by

zones: 848 °C (1121 °K), 867 °C, 897 °C, 941 °C, 948 °C and 946 °C (1219 °K). The temperature ratio of the heaters, expressed in Kelvin degrees, in the sixth zone and the first is 1.0875, therefore, in the sixth zone, the temperature is 9% higher than the average temperature for the three heaters located in the first zone.

The temperature difference in the new heating system with variable spacing of heaters has become smaller (9% vs. 23%), which proves the effectiveness of this approach.

## 5 Conclusion

In the previous designs of heating systems, in which tape heaters were located on the refractory surface of the firing modules, the expanded vermiculite concentrate was constantly in contact with them. It led to blockages and the soot deposits. This, in turn, led to local overheating, melting of nichromium and furnace failure.

Because of the lower location of the heating system, inter-turn short-circuits occurred when conductive objects entered the furnace together with vermiculite concentrate.

The use of the suspended heating system, where wire heaters hang over the raw material to be fired, eliminated all these factors and significantly increased the reliability of the furnace units.

But the operation of suspended heating systems also has some peculiarities—they do not provide uniform heating of the refractory surfaces of the modules, along which the expanded vermiculite concentrate moves, and the temperatures of the heaters from the side sections of the modules to their center increase markedly.

The research of analytical models of temperature distribution, carried out in the early works of the authors, suggested that uniform heating can be provided only in heating systems with a variable interval of installation of heaters.

The research carried out in this work at the given values of the minimum (22 mm) and maximum (44 mm) intervals and with an increase in the heater spacing to 2 mm showed that, compared with the old heating system, the temperature difference decreased from 23 to 9%. This demonstrates the effectiveness of this approach. In addition, the difference in heating temperatures of the surface of the bases of the firing modules decreases.

In furnaces with movable base plates, the unbalance of inertial loads became another factor reducing reliability. The developed methods of their balancing, shown in the present work, make it possible to provide dynamic equilibrium of all movable parts of new furnace units.

## References

1. Ding, F., Gao, M., Wang, J., Shen, T., Zang, W.: Tuning wettability by controlling the layer charge and structure of organo-vermiculites. *J. Ind. Eng. Chem.* **57**, 304–312 (2018). <https://doi.org/10.1016/j.jiec.2017.08.037>
2. Figueiredo, S.: The influence of acid treatments over vermiculite based material as adsorbent for cationic textile dyestuffs. *Chemosphere* **153**, 115–129 (2016). <https://doi.org/10.1016/j.chemosphere.2016.03.004>
3. Mo, K.H., Lee, H.J., Liu, M.Y.J., Ling, T.C.: Incorporation of expanded vermiculite lightweight aggregate in cement mortar. *Constr. Build. Mater.* **179**, 302–306 (2018). <https://doi.org/10.1016/j.conbuildmat.2018.05.219>
4. Karatas, M., Benli, A., Toprak, H.A.: Effect of incorporation of raw vermiculite as partial sand replacement on the properties of selfcompacting mortars at elevated temperature. *Constr. Build. Mater.* **221**, 163–176 (2019). <https://doi.org/10.1016/j.conbuildmat.2019.06.077>
5. Zhang, Y.N., et al.: Development and thermochemical characterizations of vermiculite SrBr<sub>2</sub> Composite sorbents for low-temperature heat storage. *Energy* **115**, 120–128 (2016). <https://doi.org/10.1016/j.energy.2016.08.108>
6. Ahirrao, N.S., Bhosle, S.P., Nehete, D.V.: Dynamics and vibration measurements in engines. *Proc. Manuf.* **20**, 434–439 (2018). <https://doi.org/10.1016/j.promfg.2018.02.063>
7. Shyamal, S., Swartz, C.L.E.: Real-time energy management for electric arc furnace operation. *J. Process Control* **74**, 50–62 (2019). <https://doi.org/10.1016/j.jprocont.2018.03.002>
8. Nizhegorodov, A.I., Gavrilin, A.N., Moyzes, B.B.: Improving the technology for processing sungulite vermiculite conglomerates. *Bulletin of the Tomsk Polytechnic University. Geo Assets Eng.* **330(4)**, 98–109 (2019). <https://doi.org/10.18799/24131830/2019/4/230>
9. Fuks, L., Herdzik-Koniecko, I.: Vermiculite as a potential component of the engineered barriers in low- and medium-level radioactive waste repositories. *Appl. Clay Sci.* **161**, 139–150 (2018). <https://doi.org/10.1007/s13762-017-1597-3>
10. Bryanskikh, T.V., Kokourov, D.V.: Energy efficiency of electric furnaces with movable floor in firing of vermiculite concentrates of different size groups. *Refract. Ind. Ceram.* **58**, 368–373 (2017). <https://doi.org/10.1007/s11148-017-0113-0>
11. Zvezdin, A.V., Bryanskikh, T.B.: Considering adaptation of electrical ovens with unit-type releasing to peculiarities of thermal energization of mineral raw materials. *IOP Conf. Series: Mater. Sci. Eng.* **168(1)**, 012003 (2017). <https://doi.org/10.1088/1757-899X/168/1/012003>
12. Lysenko, E.N., Surzhikov, A.P., Vlasov, V.A., et al.: Synthesis of substituted lithium ferrites under the pulsed and continuous electron beam heating. *Nucl. Instrum. Methods Phys. Res., Sect. B* **392**, 1–7 (2017). <https://doi.org/10.1016/j.nimb.2016.11.042>
13. Surzhikov, A.P., Frangulyan, T.S., Ghyngazov, S.A.: A thermoanalysis of phase transformations and linear shrinkage kinetics of ceramics made from ultrafine plasmochemical ZrO<sub>2</sub>(Y)-Al<sub>2</sub>O<sub>3</sub> powders. *J. Therm. Anal. Calorim.* **115(2)**, 1439–1445 (2014). <https://doi.org/10.1007/s10973-013-3455-y>
14. Surzhikov, A.P., Pritulov, A.M., Lysenko, E.N., Sokolovskii, A.N., Vlasov, V.A., Vasendina, E.A.: Influence of solid-phase ferritization method on phase composition of lithium-zinc ferrites with various concentration of zinc. *J. Therm. Anal. Calorim.* **109(1)**, 63–67 (2012). <https://doi.org/10.1007/s10973-011-1366-3>
15. Gvozdikova, S.I., Shvartsburg, L.E.: Analysis of sources and methods for reducing noise by minimizing vibrations of engineering technological processes. *Proc. Eng.* **206**, 958–964 (2017). <https://doi.org/10.1016/j.proeng.2017.10.578>
16. Nizhegorodov, A.I., Zvezdin, A.V.: Study of an electric furnace physical model for firing vermiculite with a “zero” module. *Refract. Ind. Ceram.* **57(3)**, 246–251 (2016)
17. İşçi, S.: Intercalation of vermiculite in presence of surfactants. *Appl. Clay. Sci.* **146**, 7–13 (2017)
18. Ritz, M., Zdrávková, J., Valášková, M.: Vibrational spectroscopy of acid treated vermiculites. *Vib. Spectrosc.* **70**, 63–69 (2014). <https://doi.org/10.1016/j.vibspec.2013.11.007>

19. Contreras-Serna, J., Rivera-Solorio, C.I., Herrera-García, M.A.: Study of heat transfer in a tubular-panel cooling system in the wall of an electric arc furnace. *Appl. Therm. Eng.* **148**, 43–56 (2019). <https://doi.org/10.1016/j.applthermaleng.2018.10.134>
20. Nizhegorodov, A.I., Bryanskikh, T.B., Gavrilin, A.N., Moyzes, B.B., Gradoboev, A.V., Vavilova, G.V., Tlusty, J., Tuzikova, V.: Testing a new alternative electric furnace for vermiculite concentrates heat treatment. *Bulletin of the Tomsk Polytechnic University. Geo Assets Eng.* **329(4)**, 142–153 (2018)
21. Xu, W., Zhang, J., Zhang, R.: Application of multi-model switching predictive functional control on the temperature system of an electric heating furnace. *ISA Trans.* **68**, 287–292 (2017). <https://doi.org/10.1016/j.isatra.2017.02.001>
22. Viti, C., Hirose, T.: Thermal decomposition of serpentinite during coseismic faulting: Nanostructures and mineral reactions. *J. Struct. Geol.* **32(10)**, 1476–1484 (2010)
23. Santamaria, A., Faleschini, F., Giacomello, G., et al.: Dimensional stability of electric arc furnace slag in civil engineering applications. *J. Clean. Prod.* **205**, 599–609 (2018). <https://doi.org/10.1016/j.jclepro.2018.09.122>
24. Sutcu, M.: Influence of expanded vermiculite on physical properties and thermal conductivity of clay bricks. *Ceram. Int.* **41**, 2819–2827 (2015). <https://doi.org/10.1016/j.conbuildmat.2019.07.080>
25. Kariya, J., Ryu, J., Kato, Y.: Development of thermal storage material using vermiculite and calcium hydroxide. *Appl. Therm. Eng.* **94**, 186–192 (2016). <https://doi.org/10.1016/j.applthermaleng.2015.10.090>
26. Lozano-Lunar, A., et al.: Safe use of electric arc furnace dust as secondary raw material in selfcompacting mortars production. *J. Clean. Prod.* **211**, 1375–1388 (2019). <https://doi.org/10.1016/j.jclepro.2018.12.002>
27. Soleimanimehr, H., Nategh, M.J., Najafabadi, A.F., Zarnan, A.: The analysis of the Timoshenko transverse vibrations of workpiece in the ultrasonic vibration-assisted turning process and investigation of the machining error caused by this vibration. *Precis. Eng.* **54**, 99–106 (2018)
28. Paczkowski, T., Troszyński, A.: The effect of multidirectional vibration on electrochemical machining. *Proc. Manuf.* **22**, 41–48 (2018). <https://doi.org/10.1016/j.promfg.2018.03.008>
29. Wang, Zh., Zhang, J.: Existence of periodic solutions for a class of damped vibration problems. *CR MATH* **356(6)**, 597–612 (2018). <https://doi.org/10.1016/j.amc.2008.10.020>
30. Redko, V.V., Starikova, N.S., Redko, L.A., Vavilova, G.V.: Determination of sensitivity for in-process control of cable product insulation. *IOP Conf. Ser.: Mater. Sci. Eng.* **81(1)**, 012083 (2015). <https://doi.org/10.1088/1757-899X/81/1/012083>